CELL BIOLOGY

In vivo–mimicking microfluidic perfusion culture of pancreatic islet spheroids

Yesl Jun[1,2], JaeSeo Lee[3], Seongkyun Choi[2], Ji Hun Yang[2,4], Maike Sander[1]*, Seok Chung[2,3]*, Sang-Hoon Lee[3,5]

Copyright © 2019 The Authors, some rights reserved; exclusive licensee American Association for the Advancement of Science. No claim to original U.S. Government Works. Distributed under a Creative Commons Attribution NonCommercial License 4.0 (CC BY-NC).

Native pancreatic islets interact with neighboring cells by establishing three-dimensional (3D) structures, and are surrounded by perfusion at an interstitial flow level. However, flow effects are generally ignored in islet culture models, although cell perfusion is known to improve the cell microenvironment and to mimic in vivo physiology better than static culture systems. Here, we have developed functional islet spheroids using a microfluidic chip that mimics interstitial flow conditions with reduced shear cell damage. Dynamic culture, compared to static culture, enhanced islet health and maintenance of islet endothelial cells, reconstituting the main component of islet extracellular matrix within spheroids. Optimized flow condition allowed localization of secreted soluble factors near spheroids, facilitating diffusion-mediated paracrine interactions within islets, and enabled long-term maintenance of islet morphology and function for a month. The proposed model can aid islet preconditioning before transplantation and has potential applications as an in vitro model for diabetic drug testing.

INTRODUCTION

Diabetes mellitus (DM) is a prevalent and chronic metabolic disorder that affects approximately 347 million patients worldwide (*1*). Type 1 DM (T1DM) is characterized by autoimmune-mediated destruction of β cells in the pancreatic islets of Langerhans, leading to insulin deficiency (*2*). The pathogenesis of type 2 DM (T2DM) involves β cell dysfunction and insulin resistance that induce impaired insulin secretion and decreased insulin sensitivity (*2*). Currently, pancreatic islet transplantation is the only curative therapy for T1DM; however, there are critical problems with donor shortages and low islet graft survival (*2*). Thus, it is necessary to maintain the high quality of transplanted islets and to prevent gradual losses of islet mass. In the development of diabetic drugs for the treatment of T2DM, one of the major obstacles in drug screening is the lack of in vitro models that can capture the physiological features of the in vivo environment (*3*). The use of in vitro cell-based models has ethical and cost advantages over animal research. Therefore, to identify new treatments for both forms of DM, there is an increasing demand for developing functional pancreatic islet in vitro models in which the cellular microenvironment is more fully preserved.

Native islets in the pancreas are clustered and composed of different types of endocrine cells (α, β, δ, PP, and ε cells), which closely communicate with each other via paracrine and autocrine interactions within the islets (*4*). They are also surrounded by a capillary network that is critical for adequate glucose homeostasis (*5*). Most cells in the islet are insulin-producing β cells, which are in close proximity to endothelial cells, are aligned along blood vessels, and release insulin in response to glucose uptake by diffusion into interstitial spaces (Fig. 1A) (*5*, *6*). Thus, pancreatic islets not only interact with neighboring cells by establishing aggregates as a functional unit but also are surrounded by perfusion at an interstitial flow level.

Recent progress in microfluidic-based cell culture platforms has enabled the creation of cellular environments that mimic a number of important in vivo attributes (*7*). Microfluidics offer the advantages of versatility, minimal consumption of reagents, and enhanced efficiency over traditional macroperfusion system. Current microfluidic systems in pancreatic islet research, however, are still inadequate for long-term cultures and have several challenges for engineering in vitro islet models. The first challenge is that the size of islets varies greatly, ranging from 50 to 400 μm. Because islet microvascular structures are destroyed during the isolation process, central necrosis occurs in large islets, leading to decreased viability in vitro (*8*). In addition, the great variation in cell number per islet complicates analysis of the results. Current methods of normalization based on islet equivalency have been shown to alter results depending on the size of tested islets (*9*). Another challenge is cell damage caused by flow-induced shear stress in current microfluidic devices used for islet studies (*10*). Existing studies have not optimized proper fluidic conditions for islet culture and have mainly focused on islet characterization before transplantation by monitoring hormone secretion with high temporal resolution, lasting up to 48 hours (*7*, *11*–*14*). One study by Silva *et al.* (*15*) has focused on developing a long-term pancreatic islet-on-a-chip device by reducing shear damage; however, the experiments were conducted for only 48 hours. Therefore, a platform that supports islet function and viability long-term is an important need for research on diabetes and islet physiology.

Our approach to overcome the challenge of islet size heterogeneity is to engineer well-controlled three-dimensional (3D) islet architecture by reaggregation of single islet cells into small-sized islet spheroids (<150 μm). Several studies found that small islets have superior function compared to large islets because the former have a lower diffusion barrier and thus do not suffer from hypoxia in their central areas (*8*, *16*). We have developed concave microwells for forming size-controlled cell spheroids that promote cell-cell contacts in a 3D environment and demonstrated that islet spheroids have comparable

[1]Departments of Pediatrics and Cellular and Molecular Medicine, Pediatric Diabetes Research Center, University of California, San Diego, La Jolla, CA 92093, USA. [2]School of Mechanical Engineering, Korea University, Seoul 02841, Republic of Korea. [3]KU-KIST Graduate School of Converging Science and Technology, Korea University, Seoul 02841, Republic of Korea. [4]Next & Bio Inc., Seoul National University, Seoul 08826, Republic of Korea. [5]School of Biomedical Engineering, Korea University, Seoul 02841, Republic of Korea.
*Corresponding author. Email: sidchung@korea.ac.kr (S.C.); masander@ucsd.edu (M.S.)

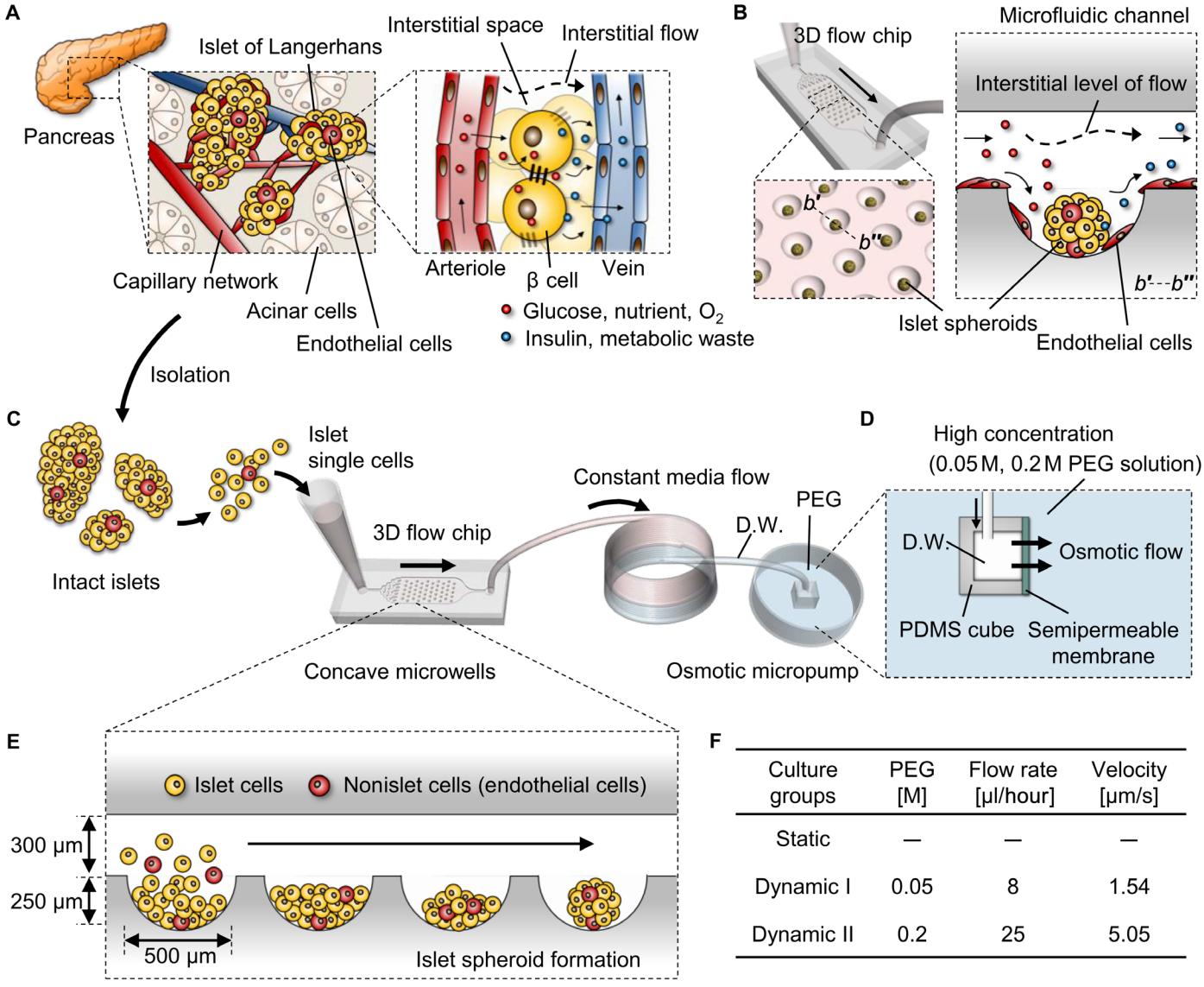

F

Culture groups	PEG [M]	Flow rate [μl/hour]	Velocity [μm/s]
Static	—	—	—
Dynamic I	0.05	8	1.54
Dynamic II	0.2	25	5.05

Fig. 1. Spheroid-based microfluidic perfusion culture of pancreatic islets to mimic the in vivo environment. (**A**) Clusters of endocrine cells dispersed throughout the exocrine acini in native pancreas form islets of Langerhans. A dense vascular network exists within islets and facilitates efficient nutrient supply and adequate responses to glucose stimulation by diffusion through extracellular spaces with interstitial level of flow. Insulin-producing β cells are tightly connected via adherent junctions to coordinate hormone release and maximize their function. (**B**) Microchip-based engineering of islet spheroids with perfusion system is reconstituted to mimic in vivo environment. Microwell arrays are homogeneously shaped and distributed, facilitating the formation of uniform-sized spheroids and enhancing cell-cell interactions. The flow chip provides continuous supply of nutrient and oxygen and removal of metabolic waste products with interstitial levels of slow flow. (**C** to **E**) Schematics of experimental setup. (C) Isolated intact islets from Sprague-Dawley rats were dispersed into single islet cells and seeded to the inlet of PDMS-based microfluidic chip. The outlet was connected to the coiled tube of an osmotic micropump. (D) The osmotic pump was dipped into the polyethylene glycol (PEG) solution to generate the main driving power of the system. D.W., distilled water. (E) The dissociated cells including islet cells and iECs aggregate and form compact spheroids in concave microwells. (**F**) Pancreatic islet cells were cultured in microfluidic chips under three different conditions: (i) static condition without micropump, (ii) dynamic I condition with a flow rate of 8 μl/hour, and (iii) dynamic II condition with a flow rate of 25 μl/hour. Both fluidic conditions (dynamics I and II) are in the range of in vivo interstitial velocities.

function and structure to intact islets (*17*). To create dynamic conditions that sustain islet function, we used in vivo–mimicking perfusion on islets using a microfluidic system that provides osmosis-driven low-speed flow (1.54 to 5.05 μm/s) comparable to in vivo interstitial flow levels of magnitude (μm/s) (*18*, *19*). The physiological slow flow with diffusion/convection balance could prevent shear damage on cells but continuously provide oxygen and nutrient supply that prolongs islet survival. With the above strategies, in this study, we aimed to explore the interstitial flow effect on 3D islet models in a microfluidic chip using reaggregated islet spheroids and concave microwell arrays integrated with an osmotic micropump (Fig. 1, B to F). The changes in islet characteristics were thoroughly investigated by comparing static and dynamic culture conditions for 2 weeks. We observed that flow enhances not only islet health but also maintenance of non-endocrine cells such as islet endothelial cells (iECs) in vitro. We optimized effective flow conditions for islet culture in our platform and

showed its potential application for drug testing. To our knowledge, our study is the first quantitative analysis of the effect of slow flow dynamic conditions on islet morphology and function under a biomimetic microenvironment and the first in vitro functional islet model that enables long-term islet maintenance for up to 1 month in a microfluidic platform. The platform can help us understand the environmental factors that support pancreatic islets, and this knowledge will provide insights into the progression of DM, improve cell preparations for clinical transplantation, and facilitate the development of novel therapeutics.

RESULTS

Survival of iECs under dynamic culture conditions

The process of islet spheroid formation is illustrated in Fig. 2A (left) and Materials and Methods. Both static and dynamic groups showed aggregation on day 1 and formed uniformly sized spheroids after day 3 inside the concave microwells, and spheroids were well maintained for 2 weeks (Fig. 2A, right). Over a month of culture, spheroids cultured under dynamic conditions, but not those cultured under static conditions, maintained their size and DNA content (fig. S1). iECs, which normally die during in vitro islet culture without endothelial cell growth supplement or extracellular matrix (ECM) (*20*), started to adhere to the flat channel under perfusion and actively expanded over time (Fig. 2A). However, iECs were not detected under static conditions (Fig. 2A). Those cells mostly expressed common endothelial markers such as von Willebrand factor (vWF) (93.7 ± 6.3%) and CD31 (79.3 ± 8.3%) (fig. S2) and therefore are considered endothelial cells. They survived on polydimethylsiloxane (PDMS)–based surfaces of both concave wells and channel bottoms, as shown in 3D projection images (Fig. 2, B and C).

We found that the iECs on flat channels increased in numbers over time under dynamic culture conditions. The percentage of endothelial cells adherent to the flat channel was proportional to the flow rate applied over microwells (Fig. 2D). The computational results of shear stress profile show that shear stress levels in flat channels were three times higher in the dynamic I (1.54 μm/s, 21.3 μPa) than in the dynamic II (5.05 μm/s, 69.9 μPa) condition (fig. S3). In addition, we investigated the effects of interstitial shear level and nutrient supply on iEC area (fig. S4). The results showed that iECs expanded on the flat channel even when exposed to nutrient-depleted conditioned medium under the dynamic I condition, as much as those with fresh medium, although islet spheroids had lower viability (fig. S4, groups 5 and 6). In contrast to the iECs that adhered to the flat channel, iECs within islet spheroids in concave wells were detected in both dynamic groups with comparable numbers of iECs (Fig. 2E). Average shear stress levels applied to spheroid surfaces were estimated to be 2.1 and 6.9 μPa for dynamics I and II, respectively, which were 10 times lower than levels in flat channels (fig. S3), indicating that surface and inside regions of spheroids were diffusion dominant, not convection dominant, compared to flat channels in both dynamic culture conditions.

Improved viability and function of islet spheroids under dynamic culture conditions

Fluorescent images of islet spheroids stained with LIVE/DEAD assay reagents show that islet spheroids in both dynamic groups remained highly viable over time, whereas many dead cells appeared on the surfaces of spheroids under static condition on day 14 (Fig. 3A). Quantification showed that the viability of cells in dynamic groups was significantly higher on both days 7 and 14 when compared to the static group (85.9 ± 7.7% and 67.8 ± 11.4%, respectively). On day 14, the cell viability under the dynamic II condition decreased from 93.1 ± 3.7% to 88.7 ± 5.9%, compared to that of dynamic I (93.4 ± 3.9% to 91.2 ± 4.9%) (Fig. 3B). To support these results, we tested the effect of dynamic culture on mRNA expression levels of apoptosis-related genes on days 7 and 14 (Fig. 3C). As controls, intact islets cultured under standard conditions for 1, 7, and 14 days were also concurrently evaluated. The expression of proapoptotic genes, *Fas* and *Bax*, increased in all groups after in vitro culture, while an antiapoptotic gene, *Bcl-2*, tended to decrease over time. However, on day 14, *Fas* and *Bax* were most highly expressed in static and intact islet groups, respectively, whereas *Bcl-2* was expressed at the lowest level in intact islets (>10-fold decrease), followed by the static group. This confirms that islet viability is improved by the dynamic culture.

To understand the effect of continuous medium flow on islet spheroids in our device, we calculated nutrient concentration patterns around a spheroid (diameter of 150 μm) using computational modeling (Fig. 3D and fig. S5). The analysis of mass transport for each of the three conditions (static, dynamic I, and dynamic II) was performed for three representative molecules in the medium: albumin, glucose, and oxygen. All three components under both dynamic conditions maintained their concentrations near initial levels within an hour by continuous supply from medium flow (fig. S5). By contrast, the concentration of these molecules drastically decreased under the static condition over time; although only 80% albumin was consumed within 24 hours, glucose and oxygen were depleted near spheroids at 5 hours and 1 hour, respectively, suggesting possible effects of the concentration gradient of these nutrients on islet function in static cultures. Islet health was then investigated by immunofluorescence staining of islet spheroids for insulin (red) and E-cadherin (green) (Fig. 3E). Confocal *z*-stacked images of spheroids revealed that insulin protein remained highly expressed throughout the culture period in dynamic groups but was barely detectable in long-term static cultures, indicating β cell dedifferentiation (*21*). In addition, compared to the static group, islets cultured under dynamic conditions had higher expression of E-cadherin, which is the cell surface protein that mediates adhesion between β cells and influences their insulin secretory capacity (*22*). Quantification of the area ratios of insulin$^+$ or E-cadherin$^+$ nuclei indicated that spheroids in static culture had 23 and 40% less insulin- and E-cadherin–expressing cells, respectively, than those in the dynamic I group on day 14 (Fig. 3F). Similar results were obtained from the analysis of cryosectioned spheroids (42 and 46% less insulin$^+$ and E-cadherin$^+$ nuclei, respectively, under the static compared to dynamic I condition on day 14) (Fig. 3, E and F).

Abundant microvilli and tight cell junctions in islet spheroids under dynamic condition with slower perfusion

The ultrastructural morphology of islet spheroids provided additional evidence for islet features being affected by the culture conditions. Comparison of scanning electron microscopy images revealed significant differences not only between static and dynamic cultures but also among different flow rates (Fig. 4, A to D). High-magnification images showed that both static and dynamic groups formed spheroids that had smooth and even surfaces with tightly connected outer cells on day 7 (Fig. 4, A and B). However, only dynamic groups had

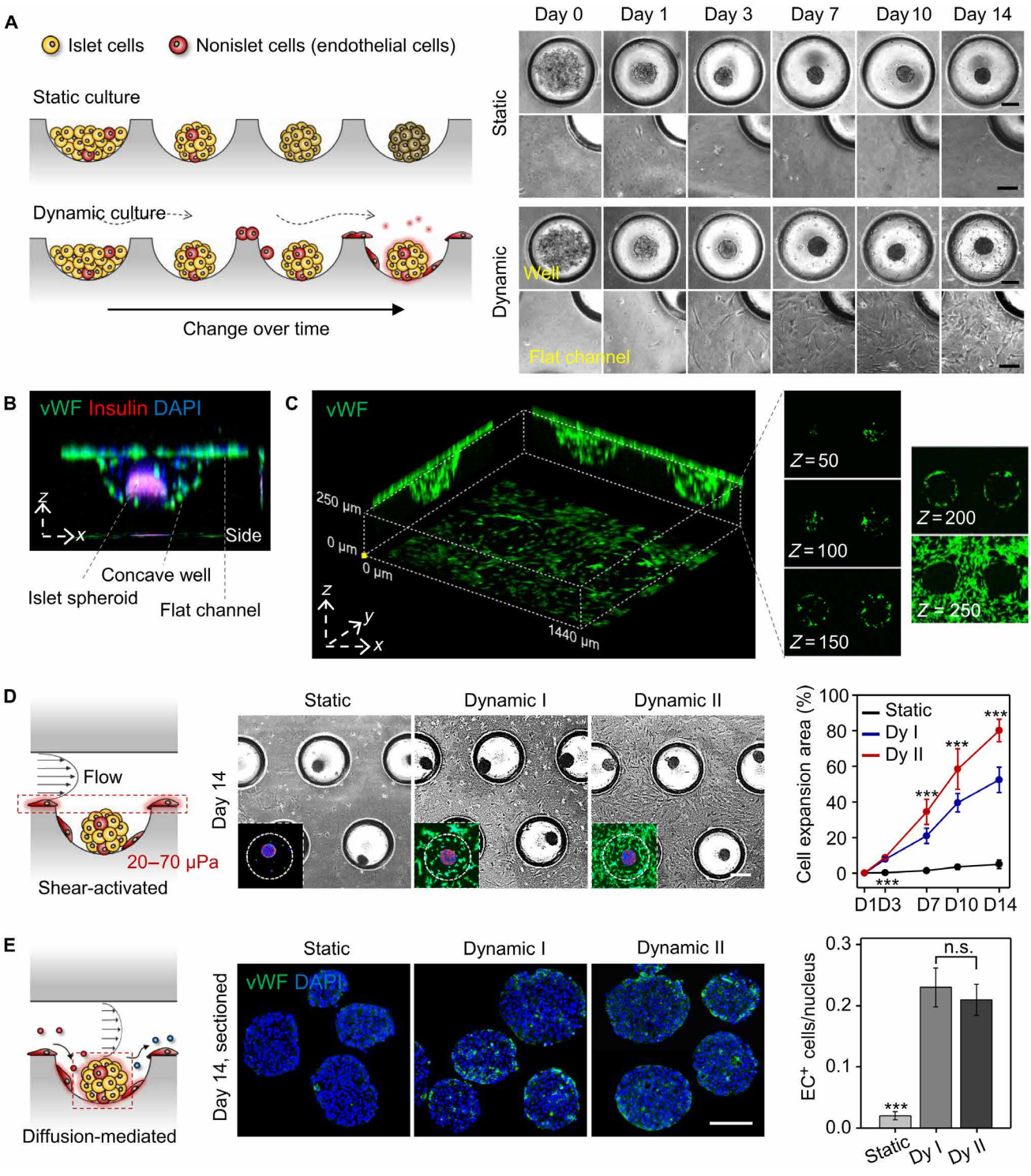

Fig. 2. Survival of iECs from islets under dynamic culture. (**A**) Morphology of islet spheroids within concave microwells and survival of iECs over time when cultured in static or dynamic culture conditions. Scale bars, 100 μm. (**B** and **C**) Detection of endothelial cell–specific markers in iECs under dynamic culture. (B) *XZ* image of a spheroid within a well containing expanded iECs. Staining for islet endocrine cells (insulin; red), endothelial cells (vWF; green), and cell nuclei [4′,6-diamidino-2-phenylindole (DAPI); blue] is shown. (C) *XY*, *YZ*, and *XZ* projection images of expanded iECs (vWF; green) on chips and *XY* images with *Z*-scan series. (**D**) Shear-activated expansion of iECs on flat channels. Morphology of iECs in different culture groups (static and dynamics I and II), immunofluorescent images (insets; insulin, red; vWF, green; DAPI, blue), and quantification of cell area on flat channels for 14 days are shown. Scale bar, 200 μm. The data are expressed as the mean ± SD ($n = 12$; $^{***}P < 0.001$ versus other groups at the same time points). (**E**) Survival of iECs within islet spheroids under diffusion-dominant microenvironment. Immunostaining of cross-sectioned islet spheroids cultured for 14 days under different culture conditions (vWF, green; DAPI, blue) is shown. Scale bar, 100 μm. The ratio of vWF^+ cells to nuclei of sectioned spheroids in static and dynamic I and II groups is shown. The data are expressed as the mean ± SD ($n = 12$; $^{***}P < 0.001$ versus dynamic groups). n.s., not significant.

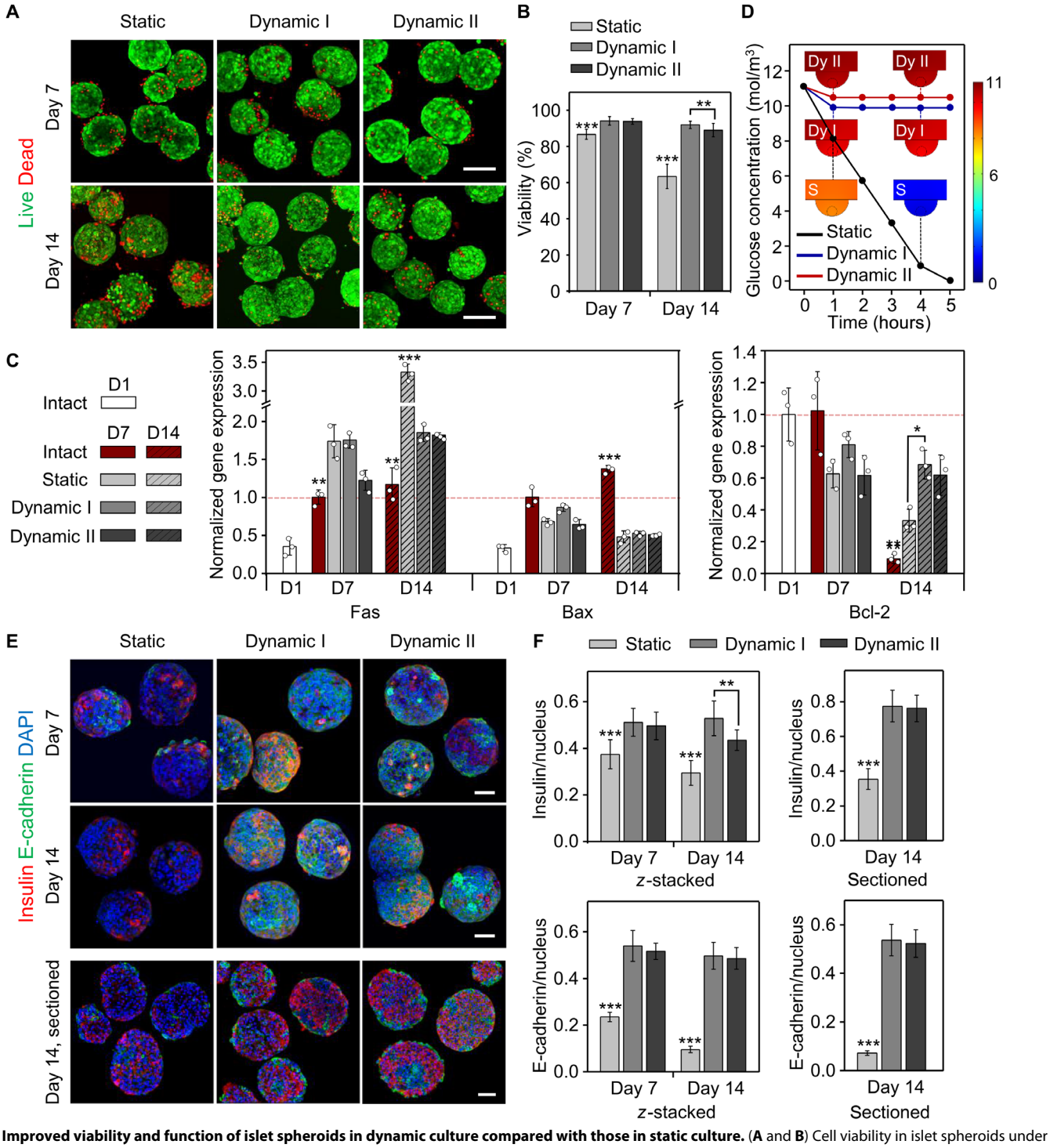

Fig. 3. Improved viability and function of islet spheroids in dynamic culture compared with those in static culture. (**A** and **B**) Cell viability in islet spheroids under static and dynamic (I and II) conditions on days 7 and 14. (A) LIVE/DEAD assay showing live cells in green and dead cells in red. Scale bars, 100 μm. (**B**) Quantification of LIVE/DEAD assay results. The data are expressed as the mean ± SD ($n = 17$; $^{**}P < 0.005$ and $^{***}P < 0.001$ versus dynamic groups). (**C**) Quantitative real-time polymerase chain reaction (qRT-PCR) analysis of proapoptotic genes, *Fas* and *Bax*, and an antiapoptotic gene, *Bcl-2*, in intact islets and islet spheroids under static and dynamic conditions in the devices over 14 days of culture. Gene expression in each group was calculated relative to the 18*S* rRNA expression and normalized to levels from intact islets at day 7. The data are expressed as the mean ± SD ($n = 3$; $^{*}P < 0.05$, $^{**}P < 0.01$, and $^{***}P < 0.001$ versus other groups at the same time point). (**D**) Mathematical simulation of glucose concentration consumed by islet spheroids in microfluidic devices under static and dynamic I and II conditions. It was assumed that the initial concentration of glucose in the medium is 11.1 mol/m^3 with a diffusion coefficient of 580 μm^2/s and a consumption rate of 0.267 mol/m^3 per second. (**E** and **F**) Immunofluorescent analysis of islet spheroids for insulin and E-cadherin on days 7 and 14. (E) Confocal *z*-stacked and cross-sectioned images of islet spheroids in different culture conditions (insulin, red; E-cadherin, green; DAPI, blue). Scale bars, 50 μm. (F) Ratio of insulin or E-cadherin to nuclei in three groups (left, *z*-stacked; right, sectioned). The data are expressed as the mean ± SD ($n = 12$; $^{**}P < 0.005$ and $^{***}P < 0.001$ versus dynamic groups).

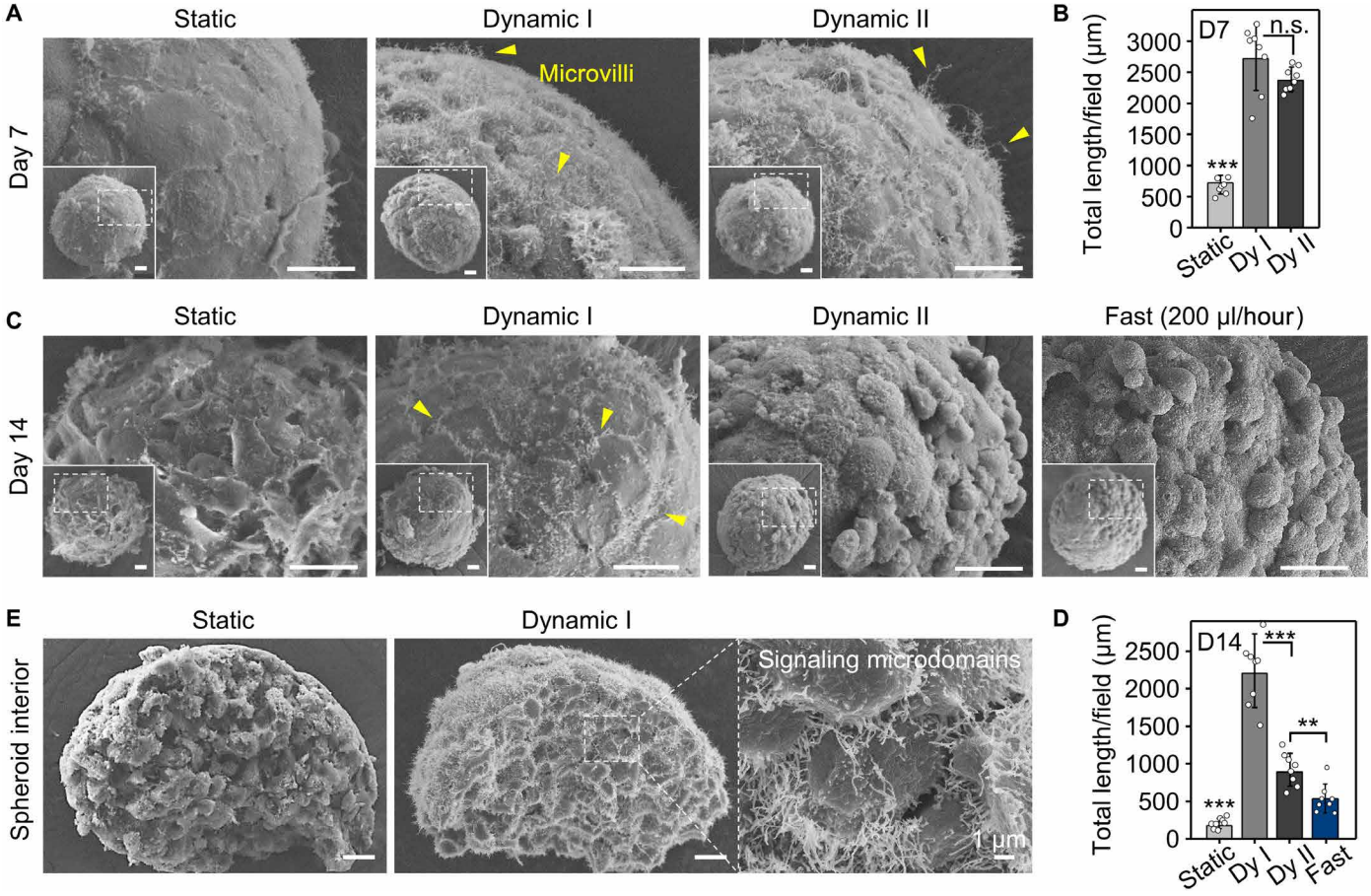

Fig. 4. Abundant microvilli and tight junctions in islet spheroids in controlled dynamic flow conditions. (**A**, **C**, and **E**) Scanning electron microscopy images of both exterior and interior of islet spheroids under static or dynamic conditions. Scale bars, 10 μm. (**B** and **D**) Total length of microvilli per field (625 μm^2) was measured in each group, as described in Materials and Methods. The data are expressed as the mean ± SD ($n = 8$; $^{**}P = 0.0035$; $^{***}P < 0.001$ versus dynamic group). (A to D) Magnified surface images show that only flow-exposed islet spheroids maintained abundant microvilli (arrowheads) on day 7. After 2 weeks, tight cell-cell junctions existed only in spheroids under dynamic I condition, whereas those under dynamic II condition lost tight connections. Both loss of tight junctions and microvilli are observed under fast fluid flow of 200 μl/hour in the device. (E) Inner structures of spheroids under static or dynamic conditions on day 7.

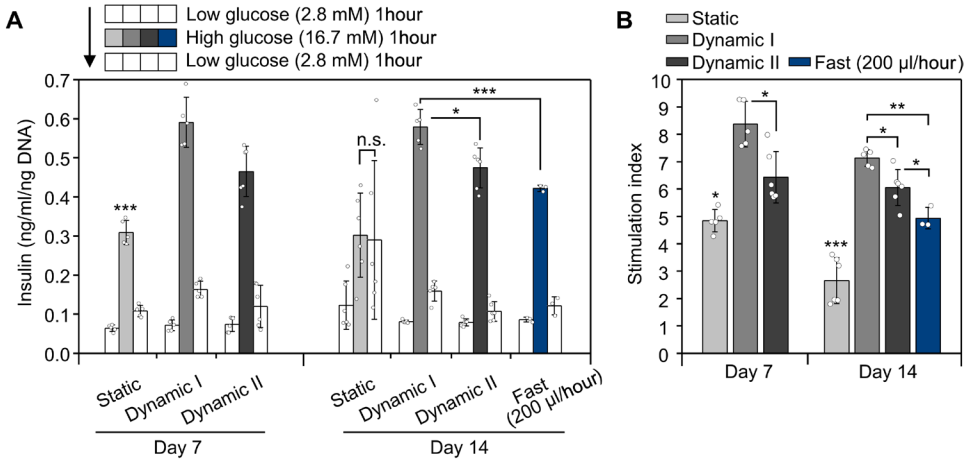

Fig. 5. Improved glucose responsiveness of islet spheroids in controlled dynamic flow conditions. (**A**) GSIS assay at low (2.8 mM) and high (16.7 mM) glucose and (**B**) stimulation index (SI) values. The amount of insulin secreted from islet spheroids in response to different glucose concentrations was measured after incubation for 1 hour with either low or high glucose. SI was calculated by dividing insulin concentrations at high and low glucose. The data are expressed as the mean ± SD ($n = 5$ for static and dynamics I and II and $n = 3$ for fast flow; $^{*}P < 0.05$, $^{**}P < 0.005$, and $^{***}P < 0.001$ versus dynamic groups at the same time point).

abundant hair-like structures called microvilli on cell surfaces. It has been reported that the microvilli are F-actin–enriched filopodia, located in the lateral cell membrane, and are enriched in glucose transporter Glut2 with an important role for sensing glucose in β cells (*23*). Analysis of the interior structure of spheroids cultured for 7 days showed that microvilli also existed at the edges of β cells under dynamic culture conditions (Fig. 4E). These functional microdomains are essential for signaling between cells and for the regulation of insulin secretion (*23*). On day 14, the static group showed the loss of tight cell-cell junctions, consistent with previous viability and immunostaining data (Fig. 4, C and D). Cells on the surface of spheroids in the dynamic II (25 μl/hour) group became rounded and lost microvilli (62.4% decrease) and contacts between neighboring cells on day 14. In contrast, spheroids in the dynamic I (8 μl/hour) group were compact with even surfaces and maintained tight cell-cell contacts and microvilli. This shows that the dynamic I condition helps maintain morphological features of native islets in long-term cultures.

Enhanced glucose responsiveness of islet spheroids under dynamic condition with slower perfusion

To determine whether the morphological changes of islets in the static and dynamic conditions correlate with functional differences, we analyzed glucose responsiveness of islet spheroids in the three groups over time. Glucose-stimulated insulin secretion (GSIS) assays were performed by sequentially incubating cells in a series of low-glucose (2.8 mM), high-glucose (16.7 mM), and low-glucose (2.8 mM) media (Fig. 5A). All three groups on day 7 showed a spike in insulin release upon exposure to high glucose, followed by a decline upon second exposure to low glucose. The static group released considerably smaller amounts of insulin when exposed to high glucose, compared to both dynamic groups at all time points. On day 14, islets in the static group failed to return to low insulin levels after a second low-glucose exposure. Notably, the dynamic I (8 μl/hour) group exhibited the highest amount of insulin release among all groups after high-glucose stimulation. To better characterize glucose responsiveness of the spheroids, we calculated the stimulation index (SI) in each sample by dividing insulin concentrations measured in high-glucose and low-glucose media (Fig. 5B). The SI values of the dynamic I group were significantly higher than those of the dynamic II group on days 7 and 14 (7.1 ± 0.3 and 6.0 ± 0.6 on day 14, respectively), indicating a decreased glucose response in the dynamic II condition. The results suggest that controlled flow rate is important for islets to improve their function under perfusion culture even with slow interstitial flow conditions. We further explored the effect of fast flow rate, which was beyond the range of interstitial levels, on islet survival and function by flowing at 200 μl/hour using a syringe pump (fig. S6). The applied flow rate was 8 times faster, and fluid shear stress that affects cells was 5.8 times higher compared with those of the dynamic II condition (fig. S6A). The fast dynamic condition resulted in decreased viability and insulin secretory function (low SI value) compared to both slow dynamic conditions (dynamics I and II) with complete loss of microvilli and fewer tight junctions between cells at the spheroid periphery (Figs. 4, C and D, and 5 and fig. S6, B and C). The viability and GSIS response of islet spheroids cultured with the flow rate above the interstitial range were better than those of islet spheroids cultured under static condition. Collectively, these results identified the dynamic I (8 μl/hour), slow perfusion condition as the most effective for maintaining islet function over a long-term culture period.

Both dynamic conditions (dynamics I and II) applied low shear stress on cells in the spheroids and exhibited similar perfusion effect on molecules in the medium (albumin, glucose, and oxygen) (fig. S5). To determine possible reasons for why spheroids in the dynamic I condition exhibit improved islet function compared to the dynamic II condition, we investigated whether the two conditions differ in the accumulation of cell-secreted molecules around the spheroids (fig. S7). We applied computational modeling and calculated the concentration of secreted molecules (insulin and glucagon) from islets using diffusion coefficient and secretion rate parameters for insulin (150 $\mu m^2/s$ and 2.1×10^{-4} mol/m^3 per second, respectively). The simulation of concentration profiles showed enriched localization of molecules near spheroids under the dynamic I condition, suggesting that the interaction with extracellular signals and neighboring cells could be enhanced compared to the dynamic II condition (fig. S7A). Hormones released from islet cells had a low Péclet number (*Pe*) around spheroids under the dynamic I condition ($Pe \approx 3$), in comparison with $Pe \approx 12$ under the dynamic II condition. Cell-secreted molecules did not transport well only by diffusion and gradually accumulated inside and around the spheroids. However, in the dynamic II condition, increased convection around the spheroid ($Pe \approx 12$) removed the secreted molecules, as shown in fig. S7A. Compared to secreted proteins, cellular toxic waste products, including lactate, ammonium, and carbon dioxide, are smaller in molecular weight and therefore had higher diffusivities (fig. S7B). The waste products quickly diffused from the cells out of the spheroids and were removed by the perfusion flow under both dynamic I and II conditions (the diffusion coefficient for waste products was set to 1500 $\mu m^2/s$) (fig. S7A).

Long-term maintenance of pancreatic islets

To determine how the culture conditions affect gene expression in islets, we compared expression levels of islet-specific genes in our in vitro models and intact islets. Specifically, isolated intact islets suspended in Petri dishes were cultured by conventional methods in the absence of flow for 7 and 14 days and compared with islet spheroids cultured in microfluidic chips under static or dynamic conditions for the same durations (Fig. 6A). As a reference, overnight-cultured fresh intact islets (day 1) were studied. All gene expression values were normalized to day 7 cultured intact islets. The results showed that β cell–enriched genes such as insulin, *Pdx1*, and *Glut2* all had significantly higher expression in dynamic groups than in intact or static groups at the same time points (Fig. 6B). The expression level of glucagon, an α cell gene, was also maintained over time in dynamic culture conditions (Fig. 6C). Numbers of nonislet cells, including endothelial cells (*Pecam*) and neurons (*Tubb3*), also increased under dynamic conditions (9.2- and 3.8-fold increase, respectively, in dynamic I versus intact islets on day 14) (Fig. 6D).

Although most β cell genes were more highly expressed in dynamic I than in dynamic II conditions, the expression of *Pecam* and *Tubb3* was comparable between dynamic groups. Because islet ECM was mostly degraded by collagenase during the islet isolation process, cultured intact islets had extremely low expression of genes encoding proteins of the ECM, which also decreased in expression over time as iECs died during in vitro culture (Fig. 6E). In contrast, collagen types IV and I, major components of islet ECM, were highly up-regulated in dynamic cultures (30.7- and 12.4-fold increase, respectively, in dynamic I versus intact islets on day 14), suggesting that surviving iECs within spheroids synthesized ECM proteins.

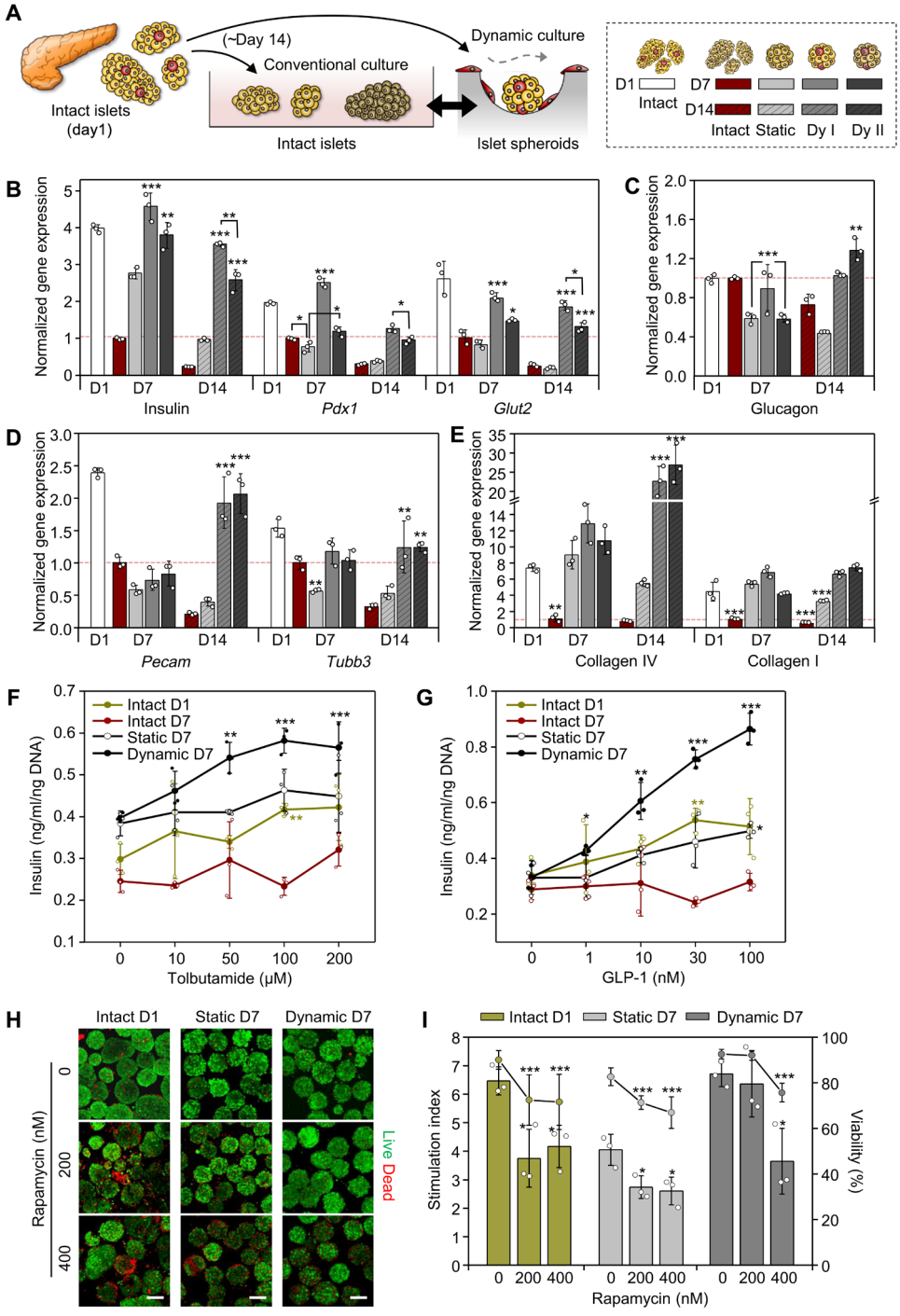

Fig. 6. Long-term maintenance of islet characteristics and application to in vitro drug testing. (**A**) Comparison of islet culture conditions; conventional suspension culture of isolated intact islets and microfluidic perfusion culture of reconstituted islet spheroids. For the following experiments, intact islets with the conventional method and islet spheroids with static and dynamics I and II were retrieved after culturing for 7 and 14 days. One-day cultured fresh intact islets were used as a reference. (**B** to **E**) qRT-PCR analysis showed higher expression of islet-specific genes in dynamic culture. Gene expression of (B) β cells (insulin, *Pdx1*, and *Glut2*), (C) α cells (glucagon), (D) nonislet cells including endothelial (*Pecam*) and neural (*Tubb3*) cells, and (E) islet ECM proteins (collagen IV and I). Gene expression in each group was calculated relative to the 18*S* rRNA expression and normalized to levels from intact islets at day 7. The data are expressed as the mean ± SD ($n = 3$; $^{*}P < 0.01$, $^{**}P < 0.005$, and $^{***}P < 0.001$ versus other groups at the same time point). (**F** and **G**) Drug efficacy testing on islet spheroids at day 7 using (F) tolbutamide and (G) GLP-1 with different dosages. The data are expressed as the mean ± SD ($n = 3$; $^{*}P < 0.05$, $^{**}P < 0.01$, and $^{***}P < 0.001$, significantly above baseline of each group). (**H** and **I**) Drug toxicity was evaluated on islet spheroids at day 7 by culturing for additional 4 days under static or dynamic conditions with culture medium containing rapamycin at different concentrations (0, 200, and 400 nM). (H) Islet viability (live cells, green; dead cells, red) and (I) glucose responsiveness upon drug exposure for 4 days. Quantified viability results are represented as line plots. Scale bars, 100 μm. The data are expressed as the mean ± SD ($n = 3$ for SI and $n = 15$ for viability; $^{*}P < 0.05$ and $^{***}P < 0.001$, significantly below baseline of each group).

These ECM proteins could contribute to islet cell survival and the maintenance of islet cell function (*5*). Islet spheroids in the static group maintained normal expression of collagen until day 7, while expression levels in intact islets declined over time. Overall, our gene expression analyses showed that dynamic culture conditions maintained islet cell function for 14 days similar to intact islets at day 1. By contrast, intact islets cultured under standard conditions and spheroids cultured under the static condition lost their molecular and functional features over time. We found that interstitial flow–mimicking dynamic culture conditions help long-term maintenance of islet spheroids up to 4 weeks (fig. S8). Central necrosis was found in large intact islets and spheroids cultured under the static condition disintegrated and displayed dead cells on their surface, whereas spheroids cultured under dynamic conditions sustained their compact spheroidal structure and viability (fig. S8A). Notably, spheroids cultured under the dynamic I condition showed 91.1 ± 1.9% viability with high SI (7.1 ± 0.3) and maintained smooth ultrastructural morphology even after 28 days (fig. S8, B to D).

Application to in vitro testing

Next, we conducted a proof-of-concept in vitro application of the developed islet spheroids for drug testing by comparing the response to regulators of insulin secretion in intact islets or spheroids cultured under static and dynamic conditions (Fig. 6, F to I). In the study, only spheroids cultured under the dynamic I condition were used as dynamic, because they showed better function compared to the spheroids cultured under the dynamic II condition. For the drug efficacy testing, two typical antidiabetic drugs, tolbutamide and GLP-1, were used in different concentrations (0, 10, 50, 100, and 200 μM and 0, 1, 10, 30, and 100 nM, respectively) that cover the range of therapeutic levels (*24*, *25*). To compare the response of islets cultured under different conditions, we exposed day 1 cultured standard intact islets, intact islets, static, and dynamic models cultured for 7 days to these drugs. Tolbutamide stimulated insulin secretion in a dose-dependent manner in the dynamic group, and the maximal value was obtained at a concentration of 100 μM in both dynamic and day 1 intact groups. However, there was no significant response to tolbutamide in day 7 intact and static groups (Fig. 6F). After GLP-1 stimulation, the maximum drug-induced insulin release from the dynamic model was at 100 nM, which was significantly higher than that in the day 1 intact islet group (Fig. 6G). All groups, except for day 7 intact islets, displayed dose-dependent increases in insulin release. Thus, it is likely that spheroid culture, especially under the dynamic condition, improves sensitivity of responses to tested drugs with a pattern of insulin release similar to the pattern observed in vivo (*25*, *26*).

For drug toxicity testing, we exposed the islet models to rapamycin, which has been used in islet transplantation as an immunosuppressant. Several studies have provided clinical evidence of rapamycin β cell toxicity and investigated its direct effects on β cell survival and insulin sensitivity (*27*). We incubated static and dynamic groups cultured for 7 days under static or dynamic conditions for an additional 4 days in culture medium containing rapamycin with different concentrations (0, 200, and 400 nM). As a control, overnight-cultured intact islets were also evaluated. After exposure for 4 days, all islet models showed decreased survival and function over time, but different resistance responses to toxicity were found among groups (Fig. 6, H and I); viability and SIs in both intact and static groups decreased at 200 nM, while the dynamic group started to lose their function at 400 nM. Higher toxicity resistance in the dynamic group reflects that in vitro toxicity assays may have significantly different results depending on the culture environment. Together, we confirmed that our functional islets cultured under interstitial flow–mimicking dynamic conditions can be used for in vitro drug testing with better sensitivity and predictability than islets cultured by conventional methods.

DISCUSSION

It has been reported that isolated intact islets from normal pancreas gradually lose their integrity, viability, and function during in vitro culture because of destruction of the islet microenvironment (*28*). Many studies have focused on the incorporation of growth factors or supportive cells that promote vascularization for application in islet transplantation (*28*). Although there are numerous studies on microengineering methods for 3D pancreatic islet models to better mimic the islet in vivo environment, there have been only a few studies exploring the effect of flow (*29*). A dynamic in vitro model could more accurately replicate in vivo physiological cues and islet physiological activities. The study by Li *et al.* (*3*) demonstrated that perfused 3D culture of islets maintained islet viability and function in vitro for 7 days by using a bioreactor system. In this culture system, islets displayed a higher sensitivity to drugs compared to conventional 2D and 3D static models. Recently, two-organ-chip models have been studied by coculturing islets with liver or intestinal tissues (*30*, *31*). Although they could replicate physiological organ cross-talk in microfluidic devices, both studies did not consider potential shear damage to the peripheral cells, which could impair normal islet architecture and function in vitro. Because of the previously described challenges and complexity of maintaining primary islets in culture, there are no previous reports of culturing islet microtissues in a microfluidic chip with long-term viability and function, which would have applications for diabetic drug screening and in vivo implantation (*10*). The current study was designed to build a uniform islet microtissue with controlled sizes under optimized dynamic culture conditions to allow physiological oxygen gradients and nutrient supply by interstitial flow for effective islet culture.

Consistent with earlier studies of islets in perfusion culture (*3*), we observed functional improvement of islets in our microfluidic system when compared with static conditions (Fig. 3). We demonstrated that not only islet viability and function but also microstructure that supports islet stability and function were well maintained under dynamic culture conditions (Fig. 4). Several studies have reported the importance of islet architecture for determining β cell function, as islet compaction and cell-cell contacts are responsible for coordinated insulin secretion via synchronization of β cell activity (*32*). In islet ultrastructural studies, microvilli were found to be enriched in the surface microdomains, where key elements for cell signaling are concentrated for importing glucose and secreting insulin (*23*). Our dynamic culture models exhibited higher E-cadherin expression, tight cell-cell adhesion, and abundant microvilli compared to static models, and these distinct morphological features correlated with insulin secretory capacity (Figs. 3 to 5). This improved islet function by perfusion could be attributed to maintaining continuous nutrient and oxygen concentrations during culture in microfluidic devices, as confirmed in our simulation data (fig. S5).

The applied flow rates to the islet spheroids in our experiments were slower than those used in earlier studies (120 to 1500 μl/hour)

(*7*, *11*–*15*). Although it has been reported that islet blood flow rates are estimated to be 10 to 20 nl/ml per islet (*33*), the interstitial flow rate from blood vessels in islets is still unknown. We selected flow velocities of 1.54 and 5.05 μm/s, which were within a range of published in vivo and in vitro interstitial flow velocities (*18*, *19*), but this level has not been replicated with a syringe pump because of the significant flow oscillations at low flow rates (*7*). However, the osmotic micropump developed by Park *et al.* (*34*) enables continuous and controllable extremely slow flow for several weeks without using any complicated instrumentation or an external power source. When we cultured islet spheroids under the fast fluid flow generated by a syringe pump (200 μl/hour) comparable to the levels that were used in previous islet studies (120 to 1500 μl/hour) (*7*, *11*–*15*), islet morphology and function were maintained significantly better than under static culture but not as well as in the slower dynamic culture groups (Figs. 4 and 5 and fig. S6), indicating that higher fluid shear causes cell damage. The study by Silva *et al.* (*15*) limited flow velocity around the islets to enhance islet function in their newly designed microfluidic chip; however, their reduced shear values (<6 mPa) were still much greater than the levels used in our flow conditions (<188 μPa) (fig. S6A). Our study introduced very slow interstitial level flow and immobilized spheroids within microwells to minimize shear damage on the spheroid periphery while still enhancing (i) continuous delivery of nutrients to islet cells and (ii) waste removal at the same time. As shown in iEC morphology in our device, iECs experienced shear-dependent proliferation only in the flat channels, indirectly proving the distribution and profile of shear stress, high shear on the flat channel and extremely low shear (<23.8 μPa) on the surface of the concave region (Fig. 2, D and E, and fig. S3). Islet spheroids in our microfluidic device received sufficient nutrients and oxygen by slow perfusion, prolonging their physiological function along with reduced shear damage.

Endocrine cells within the islet produce different hormones and closely interact with non–hormone-producing cells, including endothelial cells and autonomic neurons, which provide signals that regulate the secretory response (*4*). Endocrine cells communicate through the release of their secretory products into the interstitial fluid: Insulin inhibits glucagon secretion from α cells, glucagon stimulates insulin secretion from β cells, and somatostatin from δ cells inhibits the release of all islet hormones (*4*). This paracrine signaling in islets acts as a feedback mechanism and enables a coordinated hormonal response for maintaining blood glucose homeostasis (*35*). While the actual concentration and transport of hormones in (combined) diffusive and convective interstitial spaces within islets are still poorly understood (*35*), the local paracrine effect between endocrine cells is likely to be important for determining islet function. We found that the flow at the extremely slow interstitial rate of 8 μl/hour (1.54 μm/s, dynamic I condition) drastically improved the localization of paracrine factors, as described in simulation profiles that show higher concentration of secreted hormones near spheroids (fig. S7). When the flow rate increased only a little bit up to 25 μl/hour (5.05 μm/s, dynamic II condition), transport of the secreted molecules became mediated by convective flow ($Pe > 10$), and the local gradient of the secreted molecules disappeared by the convective flow. Thus, spheroids cultured under the dynamic I condition showed the highest glucose responsiveness and β cell–specific gene expression during the entire culture period comparable to overnight-cultured intact islets (Figs. 5 and 6B). More than 90% of the spheroids remained viable for a month (fig. S8). Moreover, we demonstrated that the extremely slow interstitial fluid flow (dynamic I) can serve as an external cue for microvilli maintenance in islets (Fig. 4). The flow range seemed to have a threshold that enhances cell-cell interaction and structural integrity of islet spheroids for effective long-term maintenance of islets in culture.

Another possible factor that affects islet function and viability was iEC survival. Within islets, β cells do not form ECM directly but instead depend on iECs to synthesize their basement membrane (*36*). ECM is an important component of the microenvironment for islet cells, as it promotes β cell survival and function via β1-integrins on the surface of β cells (*36*). ECM was most enriched in the islet spheroids cultured under dynamic conditions (Fig. 6E). While freshly isolated pancreatic islets are richly vascularized with iECs, the iECs rapidly disappear within 4 days of static culture, prohibiting the interaction between islet cells and iECs in vitro (*20*). It has been reported that iEC survival in islet spheroids is improved by dynamic culture conditions because of enhanced access of cells to albumin from the media (*14*). When the iECs left the islet spheroids, they actively migrated and expanded on the surface of the concave well and microfluidic channel as a result of flow-induced shear stress (Fig. 2D). An increase in the iEC population on the channel surface under the dynamic II condition demonstrated the favorable effect of shear stress on iEC survival. In contrast, a combination of shear stress and diffusion-mediated nutrient transport appeared to help iEC survival in or at the periphery of islet spheroids (Fig. 2D), enabling the long-term maintenance of iECs in islets for several weeks. Because it has been shown that an abnormal iEC phenotype can impair β cell function (*37*), the maintenance of iECs in our dynamic culture conditions could contribute to the observed improvement of β cell insulin secretory capacity.

The model of islet spheroids under dynamic conditions exhibited higher sensitivity to drugs compared to static and conventional models. Moreover, we showed that islet spheroids with controlled sizes had higher drug sensitivity than intact islets (Fig. 6, F and G). A recent study reported that reaggregated islets may represent a more homogeneous model for drug screening than native islets due to the size and compositional heterogeneity of native islets (*38*). For drug screening applications, the spheroids in the dynamic model can improve assay reproducibility and quality with enhanced response to therapeutics. In the field of diabetes, an in vitro platform that supports islet function and viability long-term is also an important need, as current culture techniques are unable to sustain primary islets longer than a few days. Our in vivo–mimicking microfluidic perfusion system could offer a means to sustain islets before islet transplantation and identify factors that may contribute to improved islet health. In particular, the iECs preserved within islet spheroids could increase revascularization in vivo. Furthermore, understanding the culture characteristics that support pancreatic islets will guide diabetes stem cell research, whereby our proposed model could provide a niche to facilitate efficient differentiation of uncommitted cells toward the β cell lineage or aid β cell maturation.

MATERIALS AND METHODS

Fabrication of fluidic chips with concave microwells

We previously described the fabrication of microfluidic chips integrated with concave wells for 3D perfusion culture (*39*). PDMS-based concave microwells (50 wells per chip; diameter, 500 μm; height, 250 μm) were fabricated using soft lithography techniques and the

meniscus of the PDMS prepolymer. After bonding the arrayed micro wells with the plain layer with inlet and outlet holes, the complete fluidic chips were autoclaved for cell culture (channel height, 300 μm). Micropipette tips were used as medium reservoirs. For static culture, medium reservoirs were connected to both inlet and outlet ports. For dynamic culture, a continuous flow of medium at a speed comparable to that of interstitial flow was achieved by connecting an osmotic pump to the outlet of the concave chamber (Fig. 1C). Osmosis was driven by the concentration difference between pure water and a high level of 0.05 or 0.20 M polyethylene glycol (PEG), separated from water by a cellulose membrane (Fig. 1D). The average flow rate was approximately 7.89 μl/12 hours for 0.05 M PEG solution and 25.39 μl/hour for 0.20 M PEG solution.

Isolation and culture of primary pancreatic islet cells

Pancreatic islets were isolated from 8-week-old, male Sprague-Dawley rats (KOATECH, Republic of Korea) by collagenase (Roche, Germany) digestion, followed by Histopaque (Sigma-Aldrich, MO) density gradient purification (*40*). After isolation, intact islets were handpicked under a stereomicroscope and incubated for 1 day in RPMI 1640 culture medium (Gibco BRL, Grand Island, NY) supplemented with 10% fetal bovine serum (Gibco) and 1% antibiotics containing 10,000 U of penicillin and streptomycin (Gibco) at 37°C in a humidified 5% CO_2 environment. The isolated intact islets were then dispersed to single cells using trypsin. The viability of the dispersed islet cells was assessed by trypan blue exclusion (Gibco) and was found to be >90%. All animal procedures were approved by the Korea University Institutional Animal Care and Use Committee (KUIACUC-2017-20).

Cell seeding and culture of islet spheroids

The trypsin-dispersed single islet cells (4×10^5 cells per chip) were seeded into the inlet of the fluidic chips using a micropipette, allowing the cells to become trapped within the wells (Fig. 1E). Cells were evenly docked, and after 5 min of the cell seeding, a flow of culture medium was gently applied to remove cells that had not docked within the microwells. The estimated number of trapped cells was approximately 50,000 per chip, comprising 50 spheroids per chip after cultivation. The cells were then cultured with refreshment of the medium every other day for more than 14 days. Islet aggregation and spheroid formation were observed daily under a microscope. The following three groups of islet spheroids, providing different culture conditions, were used: static, islet spheroids cultured without flow (static conditions); dynamic I, islet spheroids cultured with a flow rate of 8 μl/hour (slower perfusion); dynamic II, islet spheroids cultured with a flow rate of 25 μl/hour (slow perfusion) (Fig. 1F). Mean velocities calculated using computational simulation were 1.54 and 5.05 μm/s for dynamics I and II, respectively, which are in the range of published in vivo and in vitro interstitial velocities (0.1 μm/s to a few micrometers per second) (*18*, *19*).

Cell viability

To assess viability, islet spheroids were incubated with 50 mM calcein-AM and ethidium homodimer-1 (EthD-1; 25 mg/ml; Molecular Probes, USA) in culture medium for 40 min at 37°C and then imaged under a confocal microscope (Olympus, Japan). The calcein-AM (green) signal was taken as representing live cells, while the EthD-1 (red) signal was taken as indicating dead cells. For quantification of cell viability, the acquired images were analyzed using the ImageJ software (National Institutes of Health, Bethesda, MD).

Scanning electron microscopy

Spheroids were fixed with 2.5% glutaraldehyde in deionized water for 1 hour and then gently washed three to five times with deionized water. For secondary fixation, the spheroids gathered from concave microwells were immersed in 1% osmium tetroxide in deionized water for 1 hour. The fixed spheroids were subsequently dehydrated with a graded ethanol series (25, 50, 75, 95, and 100%), immersed in tetra butyl alcohol (three times, 30 min each) at room temperature, and then frozen at −70°C. The tetra butyl alcohol was evaporated by freeze-drying of the spheroids, which were then mounted on specimen stubs with graphite paste, coated with palladium alloy, and observed under a scanning electron microscope (JEOL Ltd., Tokyo, Japan). For quantification of the length of microvilli, the acquired images were analyzed using ImageJ. Microvilli signals in individual fields (625 μm^2) were highlighted by the intensity threshold and skeletonized using the AnalyzeSkeleton plugin. The total length of microvilli was calculated by summation of the individual branch length of skeletonized microvilli per field.

Immunofluorescence staining

Spheroids were fixed in 4% paraformaldehyde (PFA) for 30 min at 4°C, retrieved from microwells, and then incubated in 0.1% Triton X-100 in phosphate-buffered saline (PBS) for 20 min at room temperature. After incubation with 3% (w/v) bovine serum albumin (BSA) at room temperature for 30 min, the cells were incubated overnight at 4°C with appropriately diluted primary mouse anti-insulin (Abcam) and rabbit anti–E-cadherin (Santa Cruz Biotechnology). Appropriate secondary antibodies using Alexa Fluor 488–conjugated anti-rabbit immunoglobulin G or Alexa Fluor 594–conjugated immunoglobulin G secondary antibodies (Invitrogen, CA) were applied for 1.5 hours at room temperature. For sectioned spheroid staining, spheroids were fixed with 4% PFA for 30 min at 4°C, immersed overnight in 20% sucrose in PBS at 4°C, and then embedded in optimum cutting temperature compound (Tissue-Tek; Sakura Finetek, Japan). Cryostat sections (10 μm) were sliced, collected on adhesive microscope slides (Marienfeld, Germany), rinsed several times with PBS, and incubated with 3% BSA at room temperature for 30 min. The prepared specimens were incubated overnight at 4°C with primary mouse anti-insulin (Abcam), rabbit anti–E-cadherin (Santa Cruz Biotechnology), or rabbit anti-vWF (Abcam), followed by appropriate secondary antibodies. For iEC staining, adherent cells were fixed within fluidic chips and incubated with primary rabbit anti-vWF (Abcam), mouse anti-CD31 (Millipore), rabbit anti–collagen I (Abcam), or Alexa Fluor 596–conjugated phalloidin (F-actin) (Invitrogen), followed by appropriate secondary antibodies. Nuclei were counterstained with DAPI (4′,6-diamidino-2-phenylindole) (Invitrogen), and fluorescent images were acquired using a confocal microscope (Olympus).

Functional assessment

A GSIS assay was used to assess the responses of intact islets and spheroids to varying concentrations of glucose. First, spheroids were incubated for 1 hour in Krebs-Ringer–buffered Hepes (KRBH) (pH 7.4) with 0.1% (w/v) BSA containing 2.8 mM glucose. Then, the cells were incubated at 37°C for 1 hour in either low-glucose (2.8 mM) or high-glucose (16.8 mM) solutions. The amounts of insulin secreted into the low- and high-glucose solutions were measured using a rat insulin enzyme-linked immunosorbent assay (ELISA) kit (Alpco Diagnostics, NH). To compensate for the different numbers of islet

cells in the intact islets and spheroids, the secreted amounts of insulin were normalized with respect to the DNA content of islets measured by a CyQUANT kit (Invitrogen).

Gene analysis

Expression of target genes in islet cells was analyzed by quantitative real-time polymerase chain reaction (qRT-PCR). RNA was extracted from intact islets and spheroids using RNeasy Plus Mini Kits (Qiagen, Hilden, Germany) and synthesized to complementary DNA (cDNA) by reverse transcription using the PrimeScript 1st Strand cDNA Synthesis Kit (TAKARA, Japan) according to the manufacturer's instructions. qRT-PCR was performed using Power SYBR Green PCR Master Mix (Applied Biosystems) in the QuantStudio 6 Flex Real-Time PCR System (Applied Biosystems). The primer sequences are listed in table S1. Gene expression levels, normalized to housekeeping gene 18S ribosomal RNA (rRNA), were determined relative to intact islets cultured for 7 days.

Drug testing

To test the efficacy of diabetic drugs, tolbutamide (Sigma-Aldrich) and GLP-1 (Sigma-Aldrich) were used in our study. Stock solution of compounds was prepared in dimethyl sulfoxide (Sigma-Aldrich). First, intact islets and islet spheroids were retrieved and incubated at 37°C for 1 hour in KRBH with 0.1% (w/v) BSA containing 2.8 mM glucose. Then, the cells were incubated at 37°C for 1 hour in 11.2 mM glucose containing either tolbutamide or GLP-1 with desired concentrations after serial dilutions. The amounts of dose-dependent insulin release were measured using a rat ELISA kit. For drug toxicity testing on islet cells, intact islets and islet spheroids were cultured in RPMI 1640 culture medium in the absence and presence of rapamycin (Sigma-Aldrich) (0, 200, and 400 nM). After 4 days of culture, islets were collected and tested for cell viability and GSIS assays described above.

Numerical simulation

The computational fluidic dynamics model was conducted using the COMSOL Multiphysics 5.2 software (COMSOL Inc., Burlington, MA) to determine the velocity, wall shear stress, and molecular profiles in the concave wells. The 2D time-dependent model was constructed according to the geometry of the device (microfluidic channel with a height of 300 μm and microwells with a diameter of 500 μm and a depth of 250 μm) and an islet spheroid per microwell (a spheroid diameter of 150 μm). For the simulation, a constant flow rate at the inlet and no-slip boundary condition at the wall was assigned. Assumption of longitudinal symmetry allowed solving equations for only one-half of the channel and microwell, thus minimizing computational time. The dynamic viscosity and density of the culture medium were set to 0.000692 kg/m·s and 999.37 kg/m^3, respectively. The *Pe* numbers were calculated using standard equations and literature values of diffusion coefficients for each solute (see the Supplementary Materials for detailed references).

Statistical analysis

All experiments were repeated at least three times, and the data are presented as the mean ± SD. Statistical analysis was performed using the software Origin. The significance of between-group differences was evaluated with a two-tailed Student's *t* test or analysis of variance (ANOVA). $P < 0.05$ was considered statistically significant.

SUPPLEMENTARY MATERIALS

Supplementary material for this article is available at http://advances.sciencemag.org/cgi/content/full/5/11/eaax4520/DC1

Fig. S1. Size distribution and DNA analysis of pancreatic islet spheroids over 4 weeks of culture.
Fig. S2. Immunofluorescent detection of iECs on flow chips.
Fig. S3. Simulation of flow velocity and shear stress on channel bottom and spheroid surface.
Fig. S4. Interstitial flow effect on expansion of iECs cultured in conditioned media.
Fig. S5. Simulation of the diffusion and consumption of nutrients introduced into the culture systems.
Fig. S6. Fast flow condition beyond interstitial levels resulted in decreased viability of islet spheroids.
Fig. S7. Simulation of localized accumulation of secreted soluble factors from islet spheroids under two different dynamic conditions.
Fig. S8. Long-term culture (4 weeks) of islet spheroids in microfluidic chips.
Table S1. Primer design for qRT-PCR.
References (*41*–*51*)

View/request a protocol for this paper from *Bio-protocol*.

REFERENCES AND NOTES

1. J. D. Fernandes, K. Ogurtsova, U. Linnenkamp, L. Guariguata, T. Seuring, P. Zhang, D. Cavan, L. E. Makaroff, IDF diabetes atlas estimates of 2014 global health expenditures on diabetes. *Diabetes Res. Clin. Pract.* **117**, 48–54 (2016).
2. D. Mathis, L. Vence, C. Benoist, β-Cell death during progression to diabetes. *Nature* **414**, 792–798 (2001).
3. Z. H. Li, H. Sun, J. B. Zhang, H. J. Zhang, F. Y. Meng, Z. F. Cui, Development of in vitro 3D TissueFlex® islet model for diabetic drug efficacy testing. *PLOS ONE* **8**, (2013).
4. A. Caicedo, Paracrine and autocrine interactions in the human islet: More than meets the eye. *Semin. Cell Dev. Biol.* **24**, 11–21 (2013).
5. D. Eberhard, M. Kragl, E. Lammert, 'Giving and taking': Endothelial and beta-cells in the islets of Langerhans. *Trends Endocrinol. Metab.* **21**, 457–463 (2010).
6. G. C. Weir, S. Bonner-Weir, Islets of Langerhans: The puzzle of intraislet interactions and their relevance to diabetes. *J. Clin. Invest.* **85**, 983–987 (1990).
7. Y. Wang, J. F. Lo, J. E. Mendoza-Elias, A. F. Adewola, T. A. Harvat, K. P. Kinzer, D. Lee, M. Qi, D. T. Eddington, J. Oberholzer, Application of microfluidic technology to pancreatic islet research: First decade of endeavor. *Bioanalysis* **2**, 1729–1744 (2010).
8. K. Ramachandran, S. J. Williams, H. H. Huang, L. Novikova, L. Stehno-Bittel, Engineering islets for improved performance by optimized reaggregation in a micromold. *Tissue Eng. Part A* **19**, 604–612 (2013).
9. H. H. Huang, K. Ramachandran, L. Stehno-Bittel, A replacement for islet equivalents with improved reliability and validity. *Acta Diabetol.* **50**, 687–696 (2013).
10. F. R. Castiello, K. Heileman, M. Tabrizian, Microfluidic perfusion systems for secretion fingerprint analysis of pancreatic islets: Applications, challenges and opportunities. *Lab Chip* **16**, 409–431 (2016).
11. J. S. Mohammed, Y. Wang, T. A. Harvat, J. Oberholzer, D. T. Eddington, Microfluidic device for multimodal characterization of pancreatic islets. *Lab Chip* **9**, 97–106 (2009).
12. D. Lee, Y. Wang, J. E. Mendoza-Elias, A. F. Adewola, T. A. Harvat, K. Kinzer, D. Gutierrez, M. Qi, D. T. Eddington, J. Oberholzer, Dual microfluidic perifusion networks for concurrent islet perifusion and optical imaging. *Biomed. Microdevices* **14**, 7–16 (2012).
13. J. F. Lo, Y. Wang, A. Blake, G. Yu, T. A. Harvat, H. Jeon, J. Oberholzer, D. T. Eddington, Islet preconditioning via multimodal microfluidic modulation of intermittent hypoxia. *Anal. Chem.* **84**, 1987–1993 (2012).
14. K. S. Sankar, B. J. Green, A. R. Crocker, J. E. Verity, S. M. Altamentova, J. V. Rocheleau, Culturing pancreatic islets in microfluidic flow enhances morphology of the associated endothelial cells. *PLOS ONE* **6**, e24904 (2011).
15. P. N. Silva, B. J. Green, S. M. Altamentova, J. V. Rocheleau, A microfluidic device designed to induce media flow throughout pancreatic islets while limiting shear-induced damage. *Lab Chip* **13**, 4374–4384 (2013).
16. R. Lehmann, R. A. Zuellig, P. Kugelmeier, P. B. Baenninger, W. Moritz, A. Perren, P. A. Clavien, M. Weber, G. A. Spinas, Superiority of small islets in human islet transplantation. *Diabetes* **56**, 594–603 (2007).
17. Y. Jun, A. R. Kang, J. S. Lee, S. J. Park, D. Y. Lee, S. H. Moon, S. H. Lee, Microchip-based engineering of super-pancreatic islets supported by adipose-derived stem cells. *Biomaterials* **35**, 4815–4826 (2014).
18. W. J. Polacheck, R. Li, S. G. M. Uzel, R. D. Kamm, Microfluidic platforms for mechanobiology. *Lab Chip* **13**, 2252–2267 (2013).
19. W. Yao, Y. B. Li, G. H. Ding, Interstitial fluid flow: The mechanical environment of cells and foundation of meridians. *Evid Based Compl. Alt. Med.* **2012**, 853516 (2012).
20. D. Nyqvist, M. Köhler, H. Wahlstedt, P. O. Berggren, Donor islet endothelial cells participate in formation of functional vessels within pancreatic islet grafts. *Diabetes* **54**, 2287–2293 (2005).
21. C. Talchai, S. Xuan, H. V. Lin, L. Sussel, D. Accili, Pancreatic β cell dedifferentiation as a mechanism of diabetic β cell failure. *Cell* **150**, 1223–1234 (2012).

22. M. J. Carvell, P. J. Marsh, S. J. Persaud, P. M. Jones, E-cadherin interactions regulate β-cell proliferation in islet-like structures. *Cell. Physiol. Biochem.* **20**, 617–626 (2007).
23. E. Geron, S. Boura-Halfon, E. D. Schejter, B. Z. Shilo, The edges of pancreatic islet β cells constitute adhesive and signaling microdomains. *Cell Rep.* **10**, 317–325 (2015).
24. J. C. Henquin, Tolbutamide stimulation and inhibition of insulin release: Studies of the underlying ionic mechanisms in isolated rat islets. *Diabetologia* **18**, 151–160 (1980).
25. B. Ahren, G. Pacini, Dose-related effects of GLP-1 on insulin secretion, insulin sensitivity, and glucose effectiveness in mice. *Am. J. Physiol.* **277**, E996–E1004 (1999).
26. E. Tuduri, M. López, C. Dieguez, A. Nadal, R. Nogueiras, Glucagon-like peptide 1 analogs and their effects on pancreatic islets. *Trends Endocrin. Metab.* **27**, 304–318 (2016).
27. A. D. Barlow, M. L. Nicholson, T. P. Herbert, Evidence for rapamycin toxicity in pancreatic β-cells and a review of the underlying molecular mechanisms. *Diabetes* **62**, 2674–2682 (2013).
28. H. Alismail, S. Jin, Microenvironmental stimuli for proliferation of functional islet β-cells. *Cell Biosci.* **4**, 12 (2014).
29. B. Gao, L. Wang, S. Han, B. Pingguan-Murphy, X. H. Zhang, F. Xu, Engineering of microscale three-dimensional pancreatic islet models in vitro and their biomedical applications. *Crit. Rev. Biotechnol.* **36**, 619–629 (2016).
30. D. T. Nguyen, D. van Noort, I. K. Jeong, S. Park, Endocrine system on chip for a diabetes treatment model. *Biofabrication* **9**, 015021 (2017).
31. S. Bauer, C. Wennberg Huldt, K. P. Kanebratt, I. Durieux, D. Gunne, S. Andersson, L. Ewart, W. G. Haynes, I. Maschmeyer, A. Winter, C. Ammala, U. Marx, T. B. Andersson, Functional coupling of human pancreatic islets and liver spheroids on-a-chip: Towards a novel human ex vivo type 2 diabetes model. *Sci. Rep.* **7**, 14620 (2017).
32. S. S. Roscioni, A. Migliorini, M. Gegg, H. Lickert, Impact of islet architecture on β-cell heterogeneity, plasticity and function. *Nat. Rev. Endocrinol.* **12**, 695–709 (2016).
33. L. Jansson, A. Barbu, B. Bodin, C. J. Drott, D. Espes, X. Gao, L. Grapensparr, Ö. Källskog, J. Lau, H. Liljeback, F. Palm, M. Quach, M. Sandberg, V. Stromberg, S. Ullsten, P. O. Carlsson, Pancreatic islet blood flow and its measurement. *Ups. J. Med. Sci.* **121**, 81–95 (2016).
34. J. Y. Park, C. M. Hwang, S. H. Lee, S. H. Lee, Gradient generation by an osmotic pump and the behavior of human mesenchymal stem cells under the fetal bovine serum concentration gradient. *Lab Chip* **7**, 1673–1680 (2007).
35. P. Meda, Protein-mediated interactions of pancreatic islet cells. *Scientifica* **2013**, 621249 (2013).
36. H. Peiris, C. S. Bonder, P. T. Coates, D. J. Keating, C. F. Jessup, The β-cell/EC axis: How do islet cells talk to each other? *Diabetes* **63**, 3–11 (2014).
37. M. F. Hogan, R. L. Hull, The islet endothelial cell: A novel contributor to beta cell secretory dysfunction in diabetes. *Diabetologia* **60**, 952–959 (2017).
38. K. Ramachandran, X. Peng, K. Bokvist, L. Stehno-Bittel, Assessment of re-aggregated human pancreatic islets for secondary drug screening. *Br. J. Pharmacol.* **171**, 3010–3022 (2014).
39. S. A. Lee, Y. No da, E. Kang, J. Ju, D. S. Kim, S. H. Lee, Spheroid-based three-dimensional liver-on-a-chip to investigate hepatocyte-hepatic stellate cell interactions and flow effects. *Lab Chip* **13**, 3529–3537 (2013).
40. P. C. Guest, S. D. Arden, N. G. Rutherford, J. C. Hutton, The post-translational processing and intracellular sorting of carboxypeptidase H in the islets of Langerhans. *Mol. Cell. Endocrinol.* **113**, 99–108 (1995).
41. E. Figallo, C. Cannizzaro, S. Gerecht, J. A. Burdick, R. Langer, N. Elvassore, G. Vunjak-Novakovic, Micro-bioreactor array for controlling cellular microenvironments. *Lab Chip* **7**, 710–719 (2007).
42. G. L. Francis, Albumin and mammalian cell culture: Implications for biotechnology applications. *Cytotechnology* **62**, 1–16 (2010).
43. C. Provin, K. Takano, Y. Sakai, T. Fujii, R. Shirakashi, A method for the design of 3D scaffolds for high-density cell attachment and determination of optimum perfusion culture conditions. *J. Biomech.* **41**, 1436–1449 (2008).
44. P. Buchwald, FEM-based oxygen consumption and cell viability models for avascular pancreatic islets. *Theor. Biol. Med. Model.* **6**, 5 (2009).
45. M. E. Fleury, K. C. Boardman, M. A. Swartz, Autologous morphogen gradients by subtle interstitial flow and matrix interactions. *Biophys. J.* **91**, 113–121 (2006).
46. P. Buchwald, A local glucose-and oxygen concentration-based insulin secretion model for pancreatic islets. *Theor. Biol. Med. Model.* **8**, 20 (2011).
47. O. Hosoya, S. Chono, Y. Saso, K. Juni, K. Morimoto, T. Seki, Determination of diffusion coefficients of peptides and prediction of permeability through a porous membrane. *J. Pharm. Pharmacol.* **56**, 1501–1507 (2004).
48. M. J. Hubley, B. R. Locke, T. S. Moerland, The effects of temperature, pH, and magnesium on the diffusion coefficient of ATP in solutions of physiological ionic strength. *Biochim. Biophys. Acta* **1291**, 115–121 (1996).
49. T. A. Nielsen, D. A. DiGregorio, R. A. Silver, Modulation of glutamate mobility reveals the mechanism underlying slow-rising AMPAR EPSCs and the diffusion coefficient in the synaptic cleft. *Neuron* **42**, 757–771 (2004).
50. A. C. Ribeiro, V. M. M. Lobo, D. G. Leaist, J. J. Natividade, L. P. Veríssimo, M. C. Barros, A. M. Cabral, Binary diffusion coefficients for aqueous solutions of lactic acid. *J. Solution Chem.* **34**, 1009–1016 (2005).
51. P. D. Wagner, J. H. Jones, K. E. Longworth, Chapter 12—Gas exchange at rest and during exercise in mammals, in *Comparative Biology of the Normal Lung*, R. A. Parent, Ed. (Academic Press, ed. 2, 2015), pp.143–184.

Acknowledgments

Funding: This research was supported by the Basic Science Research Program through the National Research Foundation (NRF) of Korea (NRF-2017R1A2B3007701) and the Technology Innovation Program (10067407) funded by the Ministry of Trade, Industry and Energy (MOTIE) of Korea. M.S. was supported by NIH grant UC4DK104202. **Author contributions:** Y.J. designed, performed, and analyzed experiments and wrote the manuscript. J.L. assisted with cell preparation and chip fabrication. S.Cho. supported computational modeling and simulation. J.H.Y. advised the experiments. M.S. advised and supervised the revision of the manuscript. S.Chu. advised and wrote the manuscript. S.Chu. and S.-H.L. supervised the project. **Competing interests:** The authors declare that they have no competing interests. **Data and materials availability:** All data needed to evaluate the conclusions in the paper are present in the paper and/or the Supplementary Materials. Additional data related to this paper may be requested from the authors.

Submitted 25 March 2019
Accepted 25 September 2019
Published 27 November 2019
10.1126/sciadv.aax4520

Citation: Y. Jun, J. Lee, S. Choi, J. H. Yang, M. Sander, S. Chung, S.-H. Lee, In vivo–mimicking microfluidic perfusion culture of pancreatic islet spheroids. *Sci. Adv.* **5**, eaax4520 (2019).

ScienceAdvances

In vivo–mimicking microfluidic perfusion culture of pancreatic islet spheroids

Yesl JunJaeSeo LeeSeongkyun ChoiJi Hun YangMaike SanderSeok ChungSang-Hoon Lee

Sci. Adv., 5 (11), eaax4520. • DOI: 10.1126/sciadv.aax4520

View the article online
https://www.science.org/doi/10.1126/sciadv.aax4520
Permissions
https://www.science.org/help/reprints-and-permissions

Use of this article is subject to the Terms of service

Science Advances (ISSN 2375-2548) is published by the American Association for the Advancement of Science. 1200 New York Avenue NW, Washington, DC 20005. The title *Science Advances* is a registered trademark of AAAS.
Copyright © 2019 The Authors, some rights reserved; exclusive licensee American Association for the Advancement of Science. No claim to original U.S. Government Works. Distributed under a Creative Commons Attribution NonCommercial License 4.0 (CC BY-NC).